Aerosol and Air Quality Research

Hygroscopic Growth Factors of Sub-micrometer Atmospheric Aerosols at Four Selected Sites in Thailand

Jindarat Pariyothon[1,2], Surat Bualert[2*], Parkpoom Choomanee[2], Thitima Rungratanaubon[2], Thunyapat Thongyen[3], Narita Fakkaew[4], Chayaporn Phuetfoo [ID][2], Jitlada Phupijit[2], Wladyslaw W. Szymanski[2,5]

[1] Department of Social & Applied Science, College of Industrial Technology, King Mongkut' s University of Technology North Bangkok, Bangkok 10800, Thailand
[2] Department of Environmental Science, Faculty of Environment, Kasetsart University, Bangkok 10900, Thailand
[3] Department of Environmental Technology & Management, Faculty of Environment, Kasetsart University, Bangkok 10900, Thailand
[4] Department of Environmental Health, Faculty of Public Health, Kasetsart University, Sakon Nakhon 47000, Thailand
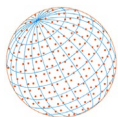[5] Faculty of Physics, University of Vienna, 1090 Vienna, Austria

ABSTRACT

Hygroscopic growth factor (Gf) of aerosols is related to water loading on particles in sub-saturated conditions. It is an essential parameter for assessing the role of atmospheric particles in the radiative transfer and cloud formation process. Therefore, the temporal variation in Gf of size-selected atmospheric particles from the Aitken mode ($D_p \leq 100$ nm) and accumulation mode ($D_p > 100$ nm) was measured using a humidified tandem differential mobility analyser (H-TDMA) and the relationship between particle size and Gf for various locations and meteorological conditions was determined. The origin of ambient particles primarily defines their properties and governs their participation in atmospheric processes. Thus, the measurements were performed in locations with different land-use types: urban, rural, coastal-industrial, and landlocked industrial areas. The data showed site-dependent patterns of temporal and spatial changes in Gf. The results indicated that the number-weighted Gf averaged over the investigated particle size range (30–250 nm) was highest in rural areas (Gf = 1.27), followed by coastal-industrial (Gf = 1.19), urban (Gf = 1.11), and landlocked industrial areas (Gf = 1.06). Particles in the urban and landlocked industrial areas had relatively low Gf values, suggesting that they originated mainly from fossil fuel combustion, in contrast to particles at other sites which can be attributed to coastal proximity.

1 INTRODUCTION

Atmospheric aerosols can be viewed as one of meteorological parameters. Their distributions are continuous and usually multi-modal, subject to the size range being investigated (e.g., Willeke and Whitby, 1975; Salma *et al.*, 2011; Hansson and Bhend, 2015). Size dependent they participate in different physico-chemical processes, ranging from interaction with solar radiation of dry particles to changes in size due to ambient humidity, which in turn modifies the optical properties of the particles, affecting radiative transfer and climate. Due to the particles' material and ambient conditions, atmospheric water vapour can be adsorbed creating under sub-saturated conditions water films of varying thicknesses. This level of interaction with water vapour and indicates that particles with a high hygroscopic growth factor (Gf) favourably participate in droplet nucleation

Special issue in honor of Prof. David Y.H. Pui for his
"50 Years of Contribution in Aerosol Science and Technology" (VI)

ORIGINAL RESEARCH
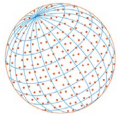https://doi.org/10.4209/aaqr.220374

and growth. If the particle composition is known, the multicomponent hygroscopic behaviour can be computed by weighing the component hygroscopicity by volume fractions in the mixture. In the absence of information on chemical particle composition, experimental data regarding the water affinity of an aerosol can be used to calculate Gf, which is the ratio of the particle size exposed to high relative humidity (RH) to the same particle size exposed to low RH (Svenningsson *et al.*, 1997; Swietlicki *et al.*, 1999, 2008; Massling *et al.*, 2005, 2009; Ye *et al.*, 2011). The values of Gf are commonly used to classify the water affinity of aerosols into following groups: near-hydrophobic (NH), less-hygroscopic (LH), more-hygroscopic (MH), and sea-salt (SS) particles, whereas the actual boundaries for these Gf groups are not uniquely defined (e.g., Vu *et al.*, 2015, 2021). A summary of pertinent data from selected past studies and from this research is shown in Table 1.

Depending on particle size and chemical composition, a certain number of fine aerosol particles under given meteorological conditions can activate to a cloud droplet serving as cloud condensation nuclei (CCN). The effectiveness of an aerosol particle to serve as a CCN depends on its size, affinity to water represented by Gf, and available atmospheric water vapour yielding in the process of heterogeneous nucleation and condensation (Petters and Kreidenweis, 2007; Swietlicki *et al.*, 2008; Coggon *et al.*, 2012). This process is governed not only by the particle size and its elemental composition but also depends on the level of external and internal mixing status of the included elements (e.g., Riemer *et al.*, 2019). Atmospheric particles are emitted from a variety of natural and anthropogenic sources, with different origins depending on human activity and land use. Consequently, the physical and chemical properties of these aerosols may significantly vary. Particles containing such ions as Na^+, K^+, Cl^-, SO_4^{2-}, and organic carbon are thought as good water adsorbers (Decesari *et al.*, 2002; Svenningsson *et al.*, 1994; Zhang *et al.*, 2007). Rural areas are often a source of particles containing inorganic compounds and tend to be more hygroscopic, whereas aerosols resulting from crop burning and combustion of fossil fuels are usually a source of carbonaceous particles with pronounced hydrophobic properties (Gu *et al.*, 2010; Keuken *et al.*, 2012). Some may be so hydrophobic that water adsorption does not occur, even at a relative humidity of 100% (Sumner, 1988; Raes *et al.*, 2000). However, the ability of these particles to attract water and act as CCN may change over time (atmospheric aging) and depend on the nature and amount of possible coating material on these particles. As these processes are quite complex and with varying environmental impacts, numerous studies on the hygroscopicity of aerosol particles have been conducted in recent years using the humidified-tandem differential mobility analyser (H-TDMA) system (e.g., Svenningson *et al.*, 1994; Swietlicki *et al.*, 2008; Massling *et al.*, 2003; Rungratanaubon *et al.*, 2017; Wu *et al.*, 2013).

In this study, particles in the Aitken mode ($D_p < 100$ nm) and accumulation mode ($D_p \geq 100$ nm) were of interest because of their important role in the processes of cloud formation and precipitation and their impact on aerosol optical properties with implications for climate (Meier *et al.*, 2009; Jiang *et al.*, 2016; Wang *et al.*, 2018; Xu *et al.*, 2020). Commonly, the types and proportions of particle distributions have different characteristics resulting from land use, human activities, and environmental conditions. Usually, it is expected that particles from the Aitken mode will

Table 1. Variability of hygroscopic growth factors of sub-micrometer atmospheric aerosols from selected studies.

Locations	%RH	Hygroscopic growth factor				Type of environment	References
		SH	NH	LH	MH		
Neuherberg (Germany)	90%	–	(1.02–1.05)	–	(1.23–1.36)	Urban	Tschiersch *et al.* (1997)
Berlin (Germany)	90%	–	–	(1.08–1.22)	(1.43–1.63)	Rural	Busch *et al.* (2002)
Beijing (China)	90%	–	(0.99–1.06)	(1.07–1.30)	(1.26–1.60)	Urban	Massling *et al.* (2009)
Shanghai (China)	91%	–	(1.03–1.09)	(1.31–1.36)	(1.40–1.68)	Urban	Ye *et al.* (2013)
Guangzhou (China)	90%	–	–	(1.11–1.16)	(1.46–1.55)	Urban	Tan *et al.* (2013)
Seoul (Korea)	90%	–	–	(1.01–1.07)	(1.26–1.43)	Urban	Kim *et al.* (2020)
London (England)	90%	< 1.00	(1.00–1.15)	(1.16–1.33)	(1.34–1.75)	Urban	Vu *et al.* (2021)
Bang Khen (Thailand)	87%	≤ 1.01	(1.01–1.10)	(1.10–1.34)	≥ 1.34	Urban	in this study
Laemphakbia (Thailand)	87%					Rural	
Maptaphut (Thailand)	87%					Industrial	
Mae Mo (Thailand)	87%					Industrial/Rural	

Special issue in honor of Prof. David Y.H. Pui for his
"50 Years of Contribution in Aerosol Science and Technology" (VI)

ORIGINAL RESEARCH
https://doi.org/10.4209/aaqr.220374

dominate the size distribution in typical urban areas, whereas in marine aerosols containing sea salt, most particles are considered to belong to the accumulation mode (Heintzenberg *et al.*, 2000).

In large urban areas, such as Bangkok, which is also true for other cities in Southeast Asia, fine particles mainly originate from anthropogenic sources, such as local traffic, local industrial plants, or transported biomass burning (Karagulian *et al.*, 2015; Choomanee *et al.*, 2020; Wang *et al.*, 2014). If they are associated with black carbon (BC) due to combustion they would likely exhibit hydrophobic behaviour. This frequently causes particles in urban areas to have low CCN potential, with Gf approximately equal to 1 (Xu *et al.*, 2020). In contrast, marine aerosols may have Gf $\gg$ 1 even at relatively low RH values (Zieger *et al.*, 2013). However, marine-type aerosols exhibit also complex size and morphology-dependent hygroscopicities (Laskina *et al.*, 2015). It is a fact of utmost significance as these particles are an important component of natural aerosols with climate implications because they act as a source of CCN (O'Dowd and de Leeuw, 2007).

A deep understanding of the climatic role of atmospheric aerosols on regional and global scales is still limited; however, it is known that they influence regional and global climate conditions (IPCC, 2013; Chakraborty *et al.*, 2021). The presence, abundance, and type of fine atmospheric particles depend on seasonal environmental conditions, geographic location, and anthropogenic activities. Moreover, time series and diurnal patterns of Gf provide insight into the possible health and environmental impacts of atmospheric aerosols (Hsiao *et al.*, 2016; Vu *et al.*, 2015; Won *et al.*, 2021). A recent large-scale study (Chen *et al.*, 2022) regarding hygroscopic growth of ambient aerosols revealed that Gf-values might increase with an aggravated air pollution problem. There, it was pointed out towards an interesting relationship of particle mass concentrations and number-weighted mean growth factors, a connection not yet entirely resolved. This work focused on the study of the hygroscopic growth factor of fine particles in areas with varying land use and human activities at four selected sites in Thailand. Temporal variations of particle fractions were linked to their Gfs and to the precipitable water content modelled with ERA-Interim Reanalysis software (https://confluence.ecmwf.int). These aspects are important because a quantitative understanding of local-scale aerosol properties and the affinity to water is a crucial to assess the atmospheric fate and transformation of aerosols, as well as their impact on local-to-regional precipitation patterns. That also would allow the examination of the role of urbanisation, land use, and agricultural practices on the regional environment and climate.

2 METHODOLOGY

2.1 Measurement Sites and Sequence of Data Collection

For this study, four different locations were selected: an urban area (Bangkok, S1), a rural area with a mangrove forest (Laemphakbia, S2), a coastal industrial area (Maptaphut industrial estate, S3), and a landlocked industrial area (Mae Moh, S4). The locations of the measuring stations and surrounding land use are shown in Fig. 1.
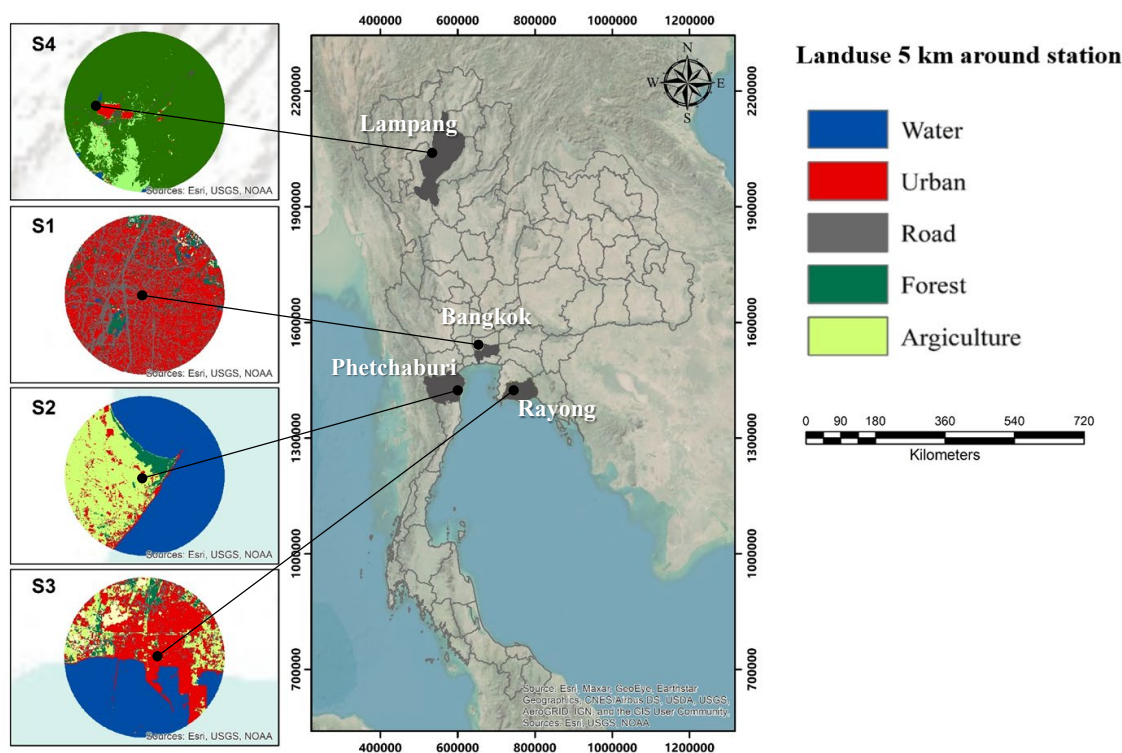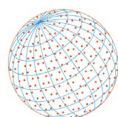
Site S1 was located on the roadside of the Chatuchak District, Bangkok (in the centre of an urban office building environment), including shopping malls and road traffic. The southern part of the site is a major road with heavy traffic, approximately 0.15 km.

Site S2 was located in the Phetchaburi Province in the western part of Thailand adjacent to the Gulf of Thailand, where the surrounding environment consists of farmland and mangrove forest at a distance from the sea coast of approximately 1.1 km in the SE direction relative to the measuring system location.

Site S3 was located within the petrochemical processing plant industrial estate area in Rayong Province in the coastal zone close to the Gulf of Thailand. The distance from the seashore in the SW direction was approximately 4.9 km.

Site S4 is located in the valley of Lampang Province, northern Thailand. This area is surrounded by high mountains, with lines of valleys oriented generally from SW to NE. Site S4 was situated about 10 km N-NE of the Mae Moh coal-fired power plant with lignite mines located about 3 km away in the WSW direction.

Aerosol measurements and a collection of meteorological data were performed in the period from 5th April to 26st May 2014. Relevant atmospheric parameters such as air temperature,

Special issue in honor of Prof. David Y.H. Pui for his
"50 Years of Contribution in Aerosol Science and Technology" (VI)

ORIGINAL RESEARCH
https://doi.org/10.4209/aaqr.220374

Fig. 1. Map of Thailand showing the study locations (S1: Bangkok; S2: Phetchaburi; S3: Rayong and S4: Lampang) and the surrounding land use.

Table 2. Details of the measuring sites, environmental data and time periods of the campaign.

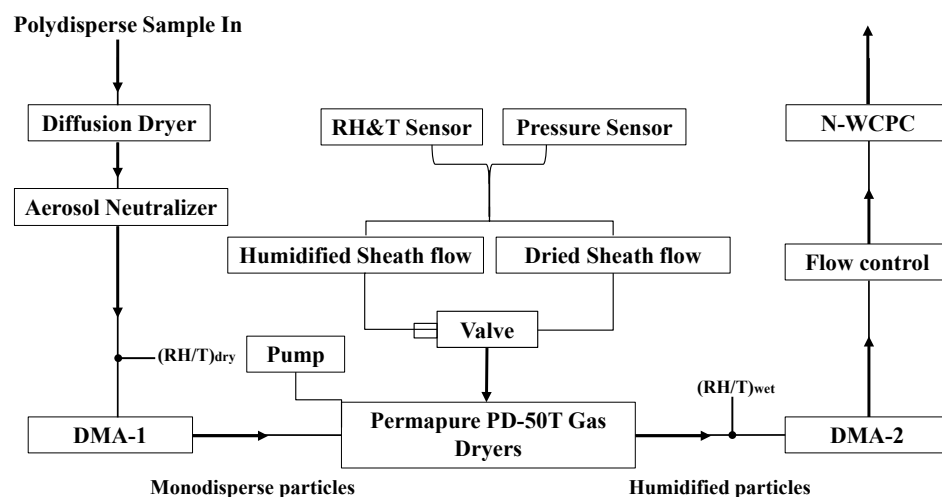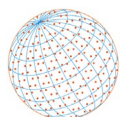| Station	Code	Latitude	Longitude	Location	Type	Sampling data	Environment data			
							WD (degree)	WS (m s^{-1})	Temp (°C)	RH (%)
Bang Khen	S1	13.826°N	100.569°E	Bangkok	Urban	21–22 May	258.54	1.56	31.59	58.41
Laemphakbia	S2	13.047°N	100.084°E	Phetchaburi Province	Rural	25–26 May	185.42	2.39	29.80	75.21
Maptaphut Industrial Estate	S3	12.915°N	100.948°E	Rayong Province	Industrial	17–18 May	215.47	1.52	29.34	78.79
Mae Moh	S4	18.426°N	99.756°E	Lampang Province	Industrial/Rural	05–06 Apr	220.97	0.76	31.59	87.50

WD: Wind Direction; WS: Wind Speed; Temp: Temperature; RH: Relative Humidity.

pressure, wind direction, wind speed, and relative humidity were determined at 10 m above the ground. The details of the location, sampling period, and environmental conditions are summarised in Table 2. All data shown in this contribution were obtained throughout 48-h per stations and averaged for three hours.

At the time of measurements, the wind speed and direction in all four study areas (S1, S2, S3, and S4) originated mainly from the SW direction. In all study areas, S1, S2, S3, and S4, the average wind speed during the measurements was 1.56, 2.39, 1.52, and 0.76 m s^{-1}, respectively.

2.2 The Measuring System: H-TDMA

Hygroscopic Tandem Differential Mobility Analyzer (H-TDMA) is a measuring system which has been applied in recent years to determine the water uptake on sub-micrometer particles at sub-saturated conditions. The H-TDMA size measurement is based on particle number concentration with unique advantages in investigating the characteristics of fine particles; thus, it has been widely used (e.g., McMurry *et al.*, 1996; Liu *et al.*, 2011; Wu *et al.*, 2016; Zhang *et al.*, 2017; Fan *et al.*, 2020).

Special issue in honor of Prof. David Y.H. Pui for his
"50 Years of Contribution in Aerosol Science and Technology" (VI)

ORIGINAL RESEARCH
https://doi.org/10.4209/aaqr.220374

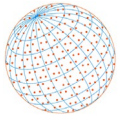**Fig. 2.** Schematic diagram of the experimental setup of the H-TDMA.

The operational parameters of the H-TDMA determine the actual measurement size range. In this work, the particle number concentrations and hygroscopic properties of fine aerosolswere investigated at particle sizes of 30, 50, 100, 150, 200, and 250 nm which is comparable with other studies (Massling *et al.*, 2005; Ye *et al.*, 2009; Massling *et al.*, 2009). A schematic diagram of the measurement system is shown in Fig. 2. Ambient aerosols enter through the sample inlet into a diffusion dryer, which defines the internal ambient low RH and dries the sample. Subsequently, particle charge equilibrium was obtained using a soft X-ray charger (Model 3081, TSI Inc.). The first differential mobility analyser (DMA-1, TSI, Model 3081L) selected quasi-monodisperse particles with a given dry size and geometric standard deviation typically < 1.2. These particles were exposed to well-defined humidity conditions using a Nafion humidifier (Perma Pure, PD-50T Gas Dryers) before entering the second DMA-2 (TSI, Model 3081L). The possible size changes of these particles can be analysed with a subsequent DMA-2, which, in combination with the nano-water-based condensation particle counter (N-WCPC, TSI, Mod. 3788), allows the number concentrations of the particles in question to be determined. The measured changes in particle size indicate the extent of hygroscopic growth, thereby elucidating the particle size-dependent Gf-values (e.g., Svenningson *et al.*, 1994; Tan *et al.*, 2013; Zhang *et al.*, 2018; Wang *et al.*, 2020).

Measurements of particle number concentrations at given sizes were performed with a time resolution of 15 min, whereas hygroscopic growth measurements of the selected dry particle diameters were repeated every 40 min. Absolute number concentration values were determined by the stability of the flowrate, which was typically of the order of $\pm 5\%$. The H-TDMA intake flow rate was fixed at 1.5 L min^{-1}. The diffusion dryer provided dry conditions at 27% $\pm$ 1% RH. Quasi-monodisperse, dry particle sizes of 30, 50, 100, 150, 200, and 250 nm were selected by applying a given fixed voltage to DMA-1 and subsequently measured by N-WCPC. Wet conditions (relative humidity (RH) = 87 $\pm$ 1%) were achieved using a Nafion humidifier. The humidified particles entered DMA-2, where the wet particle sizes ($D_{p,RH87}$) were determined, and their number concentrations measured (Chen *et al.*, 2018; Xu *et al.*, 2020). The H-TDMA system was calibrated using ammonium sulphate ((NH_4)$_2$SO$_4$), based on the extended aerosol inorganic model (E-AIM, model II) (Clegg *et al.*, 1998; Wexler and Clegg, 2002). The experimental uncertainties were comparable to those of previous studies that used the same measurement system (Mochida *et al.*, 2006; Aggarwal *et al.*, 2007; Mochida *et al.*, 2011; Boreddy *et al.*, 2014; Jing *et al.*, 2018). Further details, especially regarding the calibration, operation and principal measuring accuracy can be found elsewhere (Tan *et al.*, 2013).

3 DATA ANALYSIS AND DISCUSSION

3.1 Hygroscopic Growth of Atmospheric Particles
The affinity of particle surface towards water and its adsorption on particles at ambient temperatures and pressures may result in particle size growth at sub-saturated conditions.

Special issue in honor of Prof. David Y.H. Pui for his
"50 Years of Contribution in Aerosol Science and Technology" (VI)

ORIGINAL RESEARCH
https://doi.org/10.4209/aaqr.220374

The primary particle parameters derived from measurements with the H-TDMA as a function of particle size are the hygroscopic growth factor (Gf) and number fraction (Nf) of particles belonging to the observed groups of hygroscopic growth. Nf represents the ratio of particles belonging to a given hygroscopic mode to the total particle count.

The hygroscopic growth factor (Gf) is defined as the ratio of the particle size at high RH ($D_{p,(RH87)}$) to the particle size at low RH ($D_{p,(RH27)}$) (e.g., Massling *et al.*, 2005; Swietlicki *et al.*, 2008) and is represented by Eq. (1), as follows:

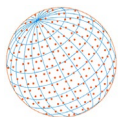$$Gf = \frac{D_{P,(RH87)}}{D_{P,(RH27)}} \tag{1}$$

where Gf is the hygroscopic growth factor [-], $D_{p,(RH87)}$ is the "wet" particle mobility diameter at high RH [nm], $D_{p,(RH27)}$ is the "dry" particle mobility diameter at low RH [nm].

3.2 Particle Number Concentrations and Growth Factors

The concentrations of ambient aerosols were measured at particle diameters of 30, 50, 100, 150, 200, and 250 nm, as shown in Fig. 3(A). There are distinctive differences between the urban area (S1) and other measuring sites. The number concentrations at S1 were approximately five-fold higher than those at S2 and S3 for all measured particle sizes. This fact was traffic-related, mirrored by the high amount of Aitken particles (Meier *et al.*, 2009). The measuring sites S2 and S3 exhibited relatively low numbers of aerosols experiencing no traffic (S2) or limited traffic (S3). Because both sites are in the coastal region, differential heating of the atmosphere usually results in dilution of aerosols due to the horizontal air movement. The landlocked S4 measuring site was exposed to aerosols originating from the coal-fired power plant and from biomass burning in this area. This was also inferred from the different shapes shown by the particle number size distribution at this location, with a maximum in the range of 150–200 nm.
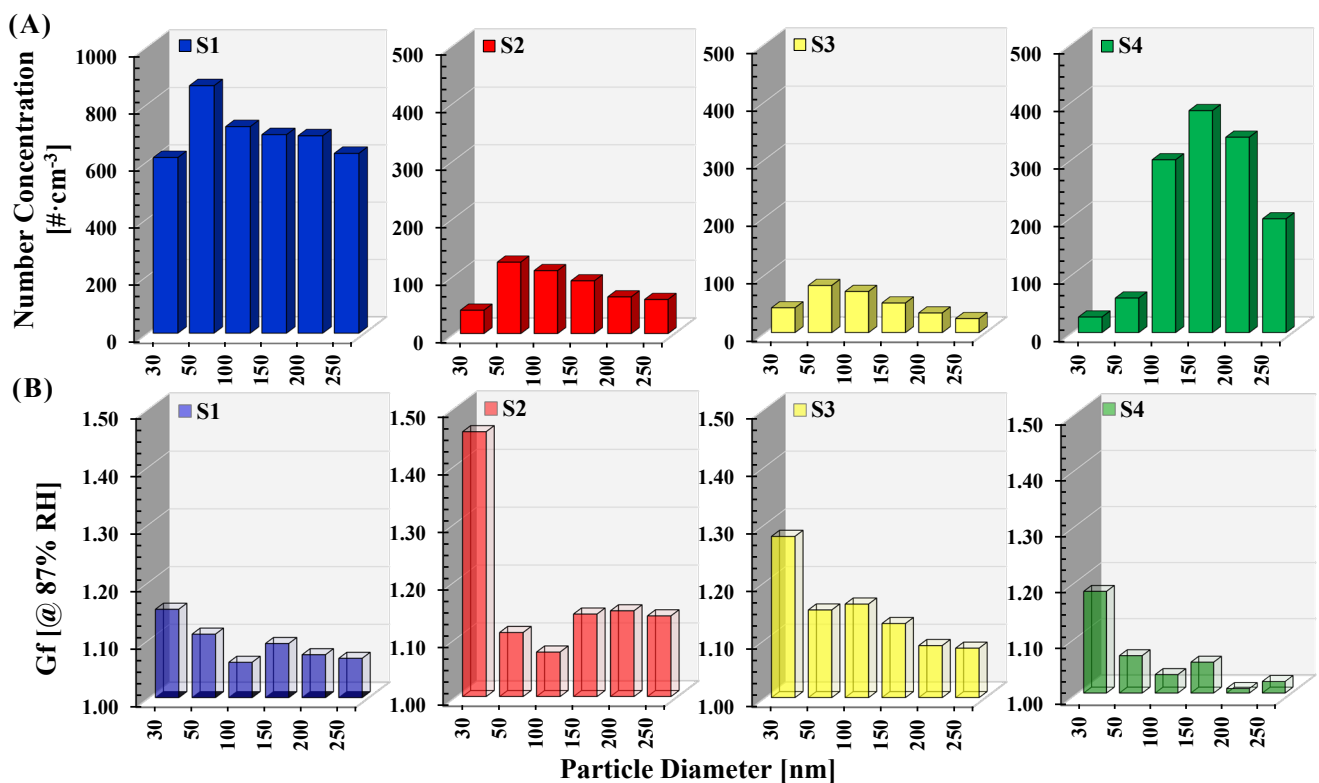

Fig. 3. (A) The mean values of particle number concentrations for all sites (S1: Bangkok; S2: Phetchaburi; S3: Rayong and S4: Lampang) and (B) corresponding hygroscopic growth factors (Gf) as a function of particle size.
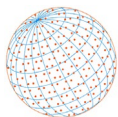
Special issue in honor of Prof. David Y.H. Pui for his
"50 Years of Contribution in Aerosol Science and Technology" (VI)

ORIGINAL RESEARCH
https://doi.org/10.4209/aaqr.220374

The corresponding hygroscopic growth factors are shown in Fig. 3(B). At site S1 there is a domination of traffic-generated particles which is confimed by the obtained Gf ≈ 1.1. This is because particles related to vehicle exhaust typically contain carbonaceous compounds, predominatly black carbon (BC) (e.g., Watson *et al.*, 2005; Tunguraiwan, 2009; Sakamoto *et al.*, 2015). In particular, the site S1 was located near roads with substantial traffic, resulting in ambient particles at this site containing a high concentration of BC as was reported elsewhere (Choomanee *et al.*, 2020). Aerosol particles at the site S4 also exhibited relatively low Gf values. This is understandable because coal combustion at this site must produce a considerable amount of hydrophobic soot and metallic trace elements.

The average Gf at a particle size of 30 nm was the highest in all study areas and decreased as the particle size increased within the Aitken mode. Gf increased again for the accumulation-mode particles (D_p = 150–250 nm), similar to that observed in earlier studies (Massling *et al.*, 2009; Ye *et al.*, 2011). The data at locations S2 and S3 show that the particles at these sites exhibited higher Gf values than those at the other two sites. Sites S2 and S3 are located next to the sea; hence, particles at these locations may contain ions such as Na^+, Mg^{2+}, and Cl^- which have high water affinity (McMurry, 2000). The Gfs measured at all stations as a function of the particle number fraction for each particle size are shown in Fig. 4 and Table 3. Usually, all particles with Gf < 1.11 are considered nearly-hydrophobic (NH) (Swietlicki *et al.*, 2008). In this study, we split the measured Gf values from the customary NH group into two groups: strongly-hydrophobic (SH, Gf ≤ 1.01) and nearly-hydrophobic (NH, Gf = 1.01–1.10), followed by the less-hygroscopic group (LH, 1.10 ≤ Gf ≤ 1.34). The objective of the insertion of Gf ≤ 1.01, representing SH particles, was to obtain somewhat finer gradation of the measured water affinity of aerosols in question. This reasoning is based on the hygroscopic growth theory developed for undersaturated conditions (Petters and Kreidenweis, 2007). From this model, the number of water monolayers on the surface of a particle can be obtained by assuming a single water molecule with a size of 0.277 nm. Consequently, for a particle size of 50 nm in diameter, representing the centre of the Aitken mode, Gf = 1.01 results in slightly less than one monolayer of water surface coverage. Gf = 1.11 for a particle size of 150 nm (which is about the centre of the accumulation mode) results in a particle surface coverage with approximately 30 monolayers of water, allowing the postulation that such a particle could likely serve as a CCN under favourable ambient conditions.
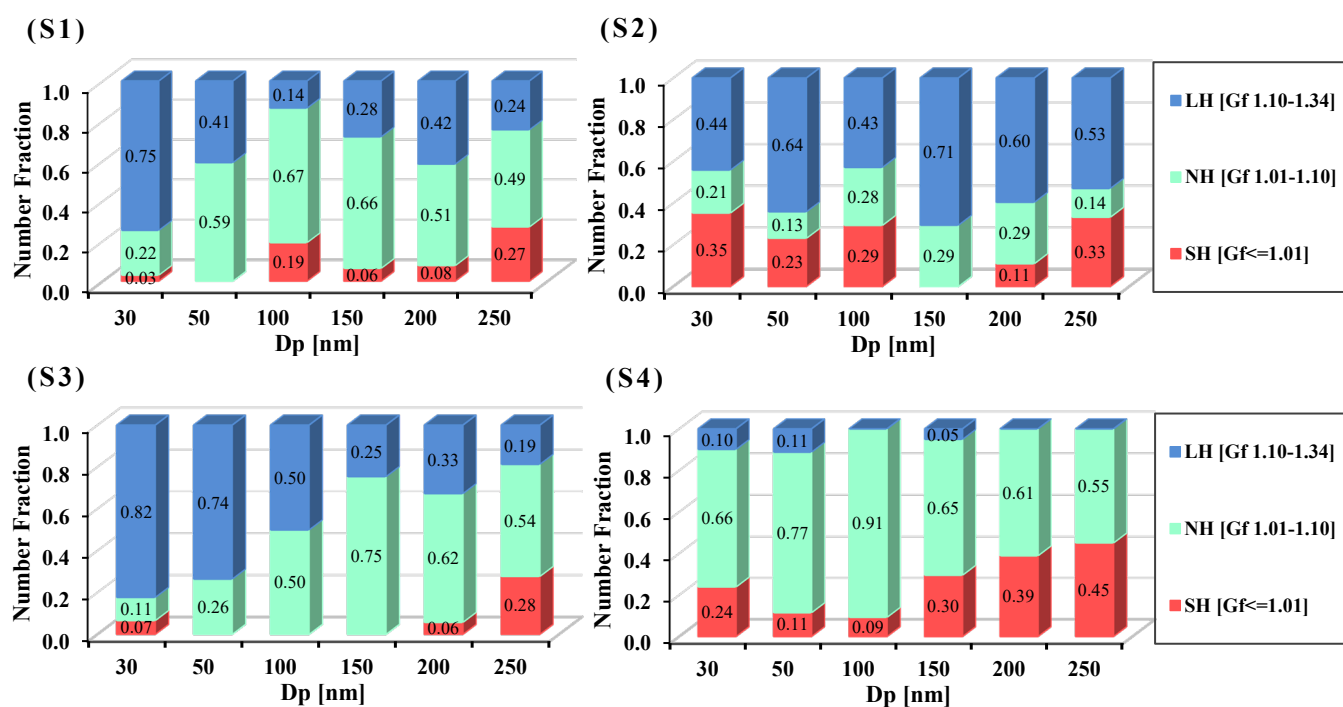
Fig. 4. Measured number fractions of ambient aerosols at the four stations (S1: Bangkok; S2: Phetchaburi; S3: Rayong and S4: Lampang) divided into following groups: strongly-hydrophobic (SH), nearly-hydrophobic (NH) and less-hygroscopic (LH).

Special issue in honor of Prof. David Y.H. Pui for his
"50 Years of Contribution in Aerosol Science and Technology" (VI)

ORIGINAL RESEARCH
https://doi.org/10.4209/aaqr.220374

Table 3. Hygroscopic growth factor and number fractions (shown in brackets) of atmospheric particles for selected particle sizes at the four measuring sites.
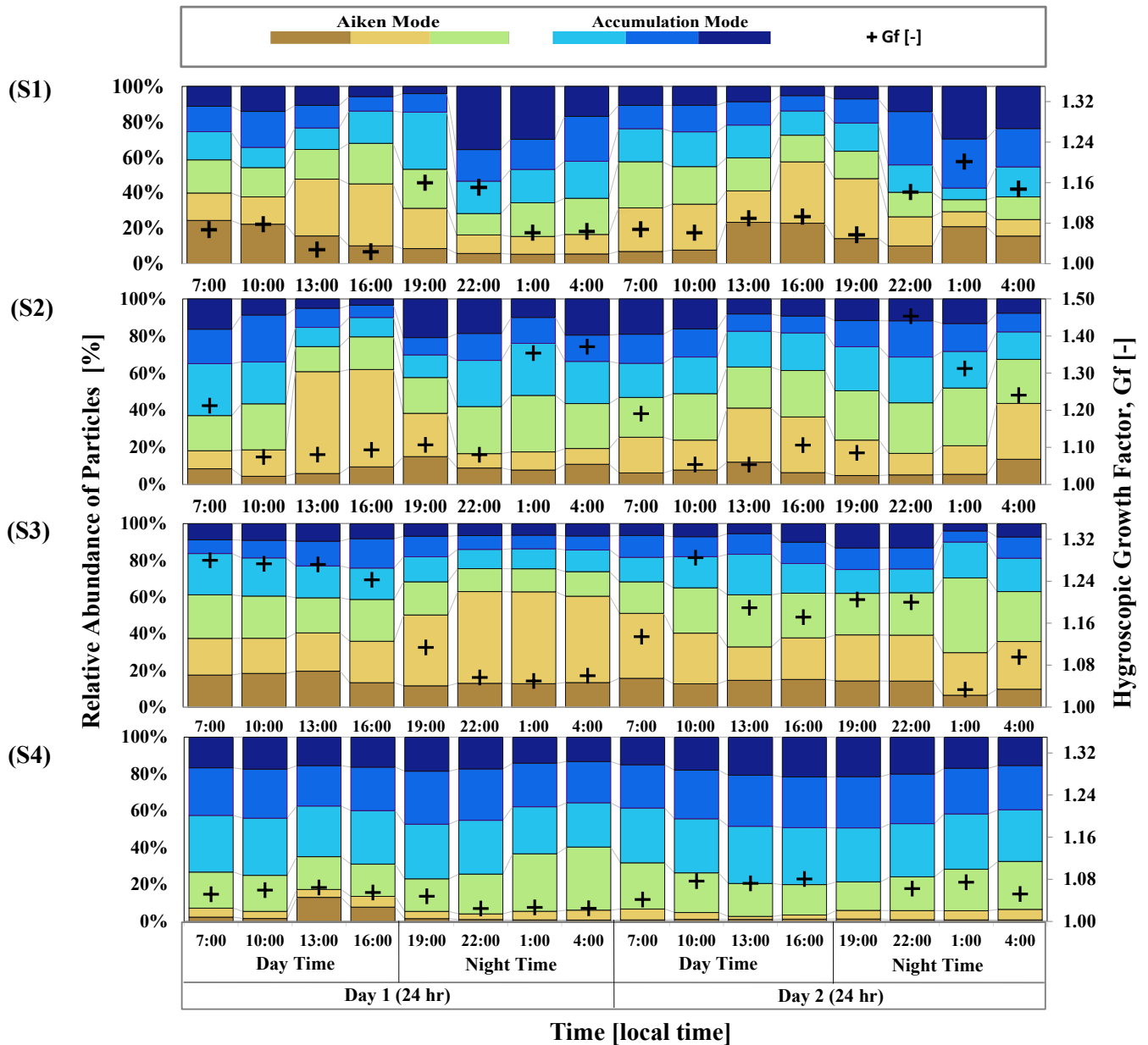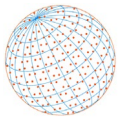
| Station | D_p (nm) | Gf (Number fraction) | | | Type of environment |
		SH ($\leq$ 1.01)	NH (1.01–1.10)	LH (1.10–1.34)	
S1	30	1.01 (0.03)	1.05 (0.22)	1.24 (0.75)	Urban aera
	50	–	1.05 (0.59)	1.20 (0.41)	
	100	1.01 (0.19)	1.06 (0.67)	1.14 (0.14)	
	150	1.01 (0.06)	1.05 (0.66)	1.18 (0.28)	
	200	1.00 (0.08)	1.06 (0.51)	1.20 (0.42)	
	250	0.95 (0.27)	1.05 (0.49)	1.37 (0.24)	
S2	30	0.91 (0.35)	1.07 (0.21)	1.75 (0.44)	Rural area
	50	0.95 (0.23)	1.06 (0.13)	1.26 (0.65)	
	100	0.91 (0.29)	1.07 (0.28)	1.18 (0.43)	
	150	–	1.07 (0.29)	1.19 (0.71)	
	200	0.99 (0.11)	1.07 (0.29)	1.21 (0.60)	
	250	0.99 (0.33)	1.07 (0.14)	1.29 (0.53)	
S3	30	1.01 (0.07)	1.03 (0.11)	1.43 (0.82)	Coastal industrial area
	50	–	1.05 (0.26)	1.24 (0.74)	
	100	–	1.05 (0.50)	1.30 (0.50)	
	150	–	1.06 (0.75)	1.31 (0.25)	
	200	1.01 (0.06)	1.05 (0.62)	1.25 (0.33)	
	250	1.01 (0.28)	1.05 (0.54)	1.28 (0.19)	
S4	30	0.99 (0.24)	1.06 (0.66)	1.12 (0.10)	Landlocked industrial/ Rural area
	50	0.99 (0.11)	1.05 (0.77)	1.16 (0.11)	
	100	1.01 (0.09)	1.04 (0.91)	–	
	150	1.01 (0.30)	1.06 (0.65)	1.14 (0.05)	
	200	1.00 (0.39)	1.04 (0.61)	–	
	250	1.01 (0.45)	1.03 (0.55)	–	

SH: Strongly-hydrophobic Gf sub-group suggested in this work), NH: Nearly-hydrophobic, LH: Less-hygroscopic, –: Data not available.

Based on the hygroscopicity boundaries stated above, it was apparent that particles at each site possessed a specific hygroscopicity-related fingerprint (Fig. 4). In all four study areas, the dominant fraction were hydrophobic particles, although the relative amounts varied significantly with the particle size and location. The boundary introduced at Gf $\leq$ 1.01 showed that at location S2, approximately 30% of the Aitken particles were strongly hydrophobic (Fig. 4). This seemingly surprising result for a measurement site (S2) practically surrounded by the mangrove area is probably due to the farmland in the SW direction at a distance of approximately 3 km, where biomass was burned. Nevertheless, owing to the proximity of the coastal area, over 55% of all measured particles at this site exhibited Gf > 1.11. In contrast, at the S4 site with not too distant coal-burning facility and wind direction toward the measuring location the hydrophobicity of particles was very pronounced in the accumulation mode, with nearly 40% of particles with Gf $\leq$ 1.01. At the urban site (S1), more than half of all measured particles had Gf < 1.1, with approximately 40% of the particles having Gf > 1.11. In contrast, data from the industrial coastal measuring site (S3) displayed the dominance of Aitken particles, with nearly 70% having Gf > 1.11. This can be attributed to the fact that the prevailing winds at this site were from the SW direction, transferring maritime air towards the measuring site.
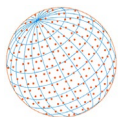
3.3 Temporal Variation of Particle Fractions and their Growth Factors

Temporal variations in the hygroscopic growth factor and changes in the relative particle number concentrations were measured over a 48-h period at all four sites and are summarised in Fig. 5. It can be seen that each site possesses a specific pattern regarding the changes in particle growth factor and size-related concentrations with daytime. Each bar represents the data averaged over 3 hrs and indicates the relative abundance of the particle number concentration for a given

Special issue in honor of Prof. David Y.H. Pui for his
"50 Years of Contribution in Aerosol Science and Technology" (VI)

ORIGINAL RESEARCH
https://doi.org/10.4209/aaqr.220374

Fig. 5. Mode-depending temporal changes in the relative abundance of particle number concentration (3 h-averages, left-side y-axis) and corresponding hygroscopic growth factors (Gf) values shown on the right-side y-axis.

size. Measurements were categorised into the Aitken mode group (D_p = 30, 50, and 100 nm) and the accumulation mode group (D_p = 150, 200, and 250 nm). The results confirmed the strong site-dependent influence of land use on the fine ambient particles. At the S1 location (urban) during the daytime period, the Aitken mode dominated the accumulation mode, with 60–70% of all particles belonging to this mode. The night-time period shows the dominance of the accumulation mode. Approximately 70% of the particles were from the accumulation mode, which was likely caused by the atmospheric ageing of aerosols. The observed Gf values indicate that daytime particles had lower hygroscopicity (Gf ≈ 1.07) which increased at night (Gf ≈ 1.15). Daytime ultrafine particles at this site mainly originated from heavy traffic and consequently coagulated and agglomerated with time, along with photochemical transformations (Salma *et al.*, 2011). As mentioned before, the Aitken mode particles at this site have likely high BC content with low water adsorption potential (Choomanee *et al.*, 2020; Xu *et al.*, 2020). The observed particle size shift to the accumulation mode with higher average Gf-values at night indicates aerosol ageing and aggregation processes (Wang *et al.*, 2014).

Special issue in honor of Prof. David Y.H. Pui for his
"50 Years of Contribution in Aerosol Science and Technology" (VI)

ORIGINAL RESEARCH
https://doi.org/10.4209/aaqr.220374

At site S2 (rural), Aitken mode particles dominated during the day, peaking in the early afternoon hours. These particles originated from agricultural activities, including crop burning, as revealed by Gf < 1.1. In contrast, at night, the growth factor continuously increased, reaching Gf > 1.3 during the 1:00–3:00 am phase, likely due to the influx of marine aerosols (Notario *et al.*, 2013) from the nearby coastal area. Consequently, this caused favourable horizontal air parcel transport. The petrochemical industrial site (S3) is located approximately 4.9 km from the coast in a southwestern direction. This site exhibited the dominance of Aitken mode particles over the entire measuring period; however, their hygroscopicity had a diurnal pattern, increasing in the morning hours up to Gf ≈ 1.3, then falling continuously from the afternoon to the minimum (Gf = 1.03) (at approximately 1:00 am) before increasing again. The observed pattern was related to the influence of terrestrial and marine winds. During the daytime, the sea breeze carries usually marine aerosols towards the land, resulting in a mixture of industrial particles and, consequently, higher average Gf values. The night-time fine particles with low Gf values were most likely emissions from industrial actions, site-related, and local traffic activities and weredominated by the particles in the Aitken mode (Zappoli *et al.*, 1999). Gfs showed a decreasing trend, reaching a minimum value at approximately 1:00 am. Site S4 (industrial, land-locked) is located in an area surrounded by mountains in the vicinity of the Mae Moh power plant. Particles in this location mainly originated from local sources, such as coal-fired power generation, lignite mining activities, and biomass burning, resulting in the dominance of particles from the accumulation mode having pronounced stable hydrophobic properties with a number-weighted average Gf = 1.06 and practically without showing any temporal pattern.
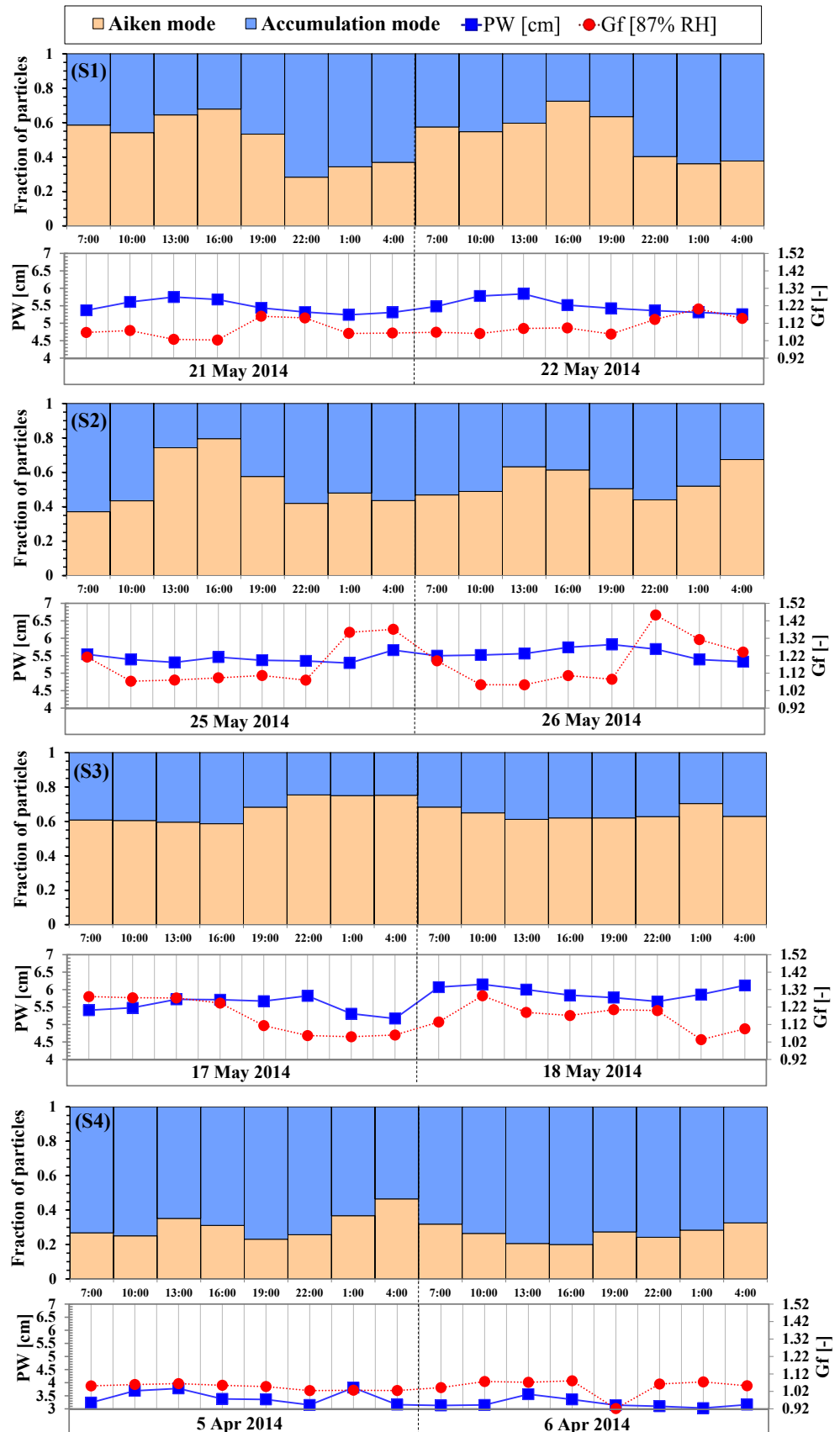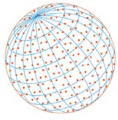
3.4 Assessing Precipitable Water Vapour Content

The interplay between fine particles and the amount of water vapour in the atmosphere results in a phase state of atmospheric aerosols. The phase state is often difficult to quantify; however, it is important to consider cloud formation via the transition of ambient particles to CCNs. Precipitable water vapor (PW) can used to diagnose the atmospheric humidity over a specific location. It is the vertically integrated amount of water vapor in the atmosphere, which is equivalent to the depth of liquid water that would result if all the water vapor in the atmospheric column would condense. Increasing amounts of ambient precipitable water (PW) could leqad to the rising number of ambient CCN. Therefore, we linked the Gf values at given particle sizes with the modelled amount of precipitable water at all measurement sites.

Many atmospheric models are not pertinent for description of small-scale processes. Therefore, reanalysis of datasets considering atmospheric temperature and precipitable water content are important for appraising the thermodynamic profiles as they could contribute to the formation of CCNs.
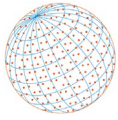
To obtain a better insight into the atmospheric situation at the measurement sites the meteorological reanalysis software (ERA-Interim Reanalysis) offered by the European Centre for Medium-Range Weather Forecasts (ECMWF) was used in this study. It is a widely employed modelling product applied in numerous climatic and atmospheric trend analysis studies (Rienecker *et al.*, 2008; Bock and Nuret, 2009; Berrisford *et al.*, 2011; Dee *et al.*, 2011; Zhang *et al.*, 2018; Buntoung *et al.*, 2020) and is available online (https://confluence.ecmwf.int).

For the appraisal of precipitable water (PW) content at the measuring sites (S1–S4) the spatial resolution of the relevant meteorological data was set to approximately 80 km (corresponding to T255 spectral resolution) on 60 levels in the vertical from the surface up to a pressure of 0.1 hPa (Berrisford *et al.*, 2011). By definition, reanalysis data are developed by revisiting the forecasts issued by regional and global climate models. Predictions for a specific time ($T_i + \Delta t$) obtained from T_i were compared with the measured data from various sources and then assimilated into the model output at a time ($T_i + \Delta t$). The model parameters were then adjusted to provide the best possible fit to the measured data at $T_i + \Delta t$, thereby providing a range of model variables that best matched the observations.

Fig. 6 shows the temporal variation in the number fraction of particles from the Aitken and accumulation modes at all four sites (S1–S4). The corresponding Gf values are presented along with the PW vapour content. The PW amount is similar at sites S1, S2, and S3, typically ranging from 5.5–6 cm, except for site S4 (industrial, landlocked), which has a PW of ~3.5 cm. This fact, together

Special issue in honor of Prof. David Y.H. Pui for his
"50 Years of Contribution in Aerosol Science and Technology" (VI)

ORIGINAL RESEARCH
https://doi.org/10.4209/aaqr.220374

Fig. 6. Averaged temporal variation of mode-related particle fractions showing the modelled associated precipitable water (PW, blue squares) amount and the hygroscopic growth factor (Gf, red dots).

Special issue in honor of Prof. David Y.H. Pui for his
"50 Years of Contribution in Aerosol Science and Technology" (VI)

ORIGINAL RESEARCH
https://doi.org/10.4209/aaqr.220374

with the very low Gf values across the investigated particle size range, indicates that the amount of CCN at this site was probably negligible. The S3 site (petrochemical industry, coastal area), with the Gf during the daytime being approximately 20% larger than that during the night-time, corresponds well with the coastal horizontal pressure gradients bringing maritime air masses towards land (enhanced by the prevailing SW wind direction). Opposing patterns can be recognised for the S2 site, which is also a coastal area but is located westward of site S3 in the Gulf of Thailand.

4 CONCLUSIONS

The amount of water uptake by fine atmospheric particles driven by their hygroscopicity is essential for predicting the role of atmospheric aerosols in radiative transfer and cloud formation processes, which are likely to have local and global impacts. Therefore, this study investigated the hygroscopic growth factor (Gf) of size-selected atmospheric particles in Aitken mode ($D_p \leq 100$ nm) and accumulation mode ($D_p > 100$ nm). Such particle growth under sub-saturated conditions must occur before atmospheric aerosols can act as CCN. Because hygroscopic particle behaviour is also linked to local land use, the hygroscopic properties of fine particles were measured at four geographically different sites. However, the data show that in addition to local sources, micrometeorological parameters influencing air mass transport determine the observed hygroscopic growth factors. The measured Gf values reported here indicate the relatively strong hydrophobic properties of the ambient particles at all sites. Therefore, a subdivision of the nearly hydrophobic particle group (Gf < 1.11) was introduced at Gf $\leq$ 1.01 to obtain a finer gradation of the measured hydrophobicity. This subdivision is based on a model representing the number of adsorbed molecular water monolayers on a particle under unsaturated conditions. The presented results indicate that substantial amounts of particles were associated with biomass and fossil fuel burning and were highly hydrophobic, with a Gf $\leq$ of 1.01.

The observed temporal variation in Gf values at urban and rural sites indicates possible land usage dependency with hygroscopic growth factors. The increasing values with time are likely caused by atmospheric aerosol ageing processes. However, at both investigated industrial sites, no such trend was observed, indicating the presence of hydrophobic industry-related particulate matter. Modelling based on the actual meteorological data and using the meteorological reanalysis software (ERA-Interim Reanalysis) for all sites during the campaign delivered the precipitable water amount, indicating sites S2 and S3 with a likelihood of CCN formation. Further such studies and the links between aerosols hygroscopicity and aggravated air pollution episodes will be addressed in future investigations because of their scientific and societal importance.
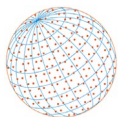
ACKNOWLEDGEMENTS
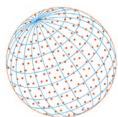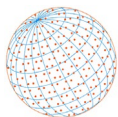
REFERENCES

Aggarwal, S.G., Mochida, M., Kitamori, Y., Kawamura, K. (2007). Chemical closure study on hygroscopic properties of urban aerosol particles in Sapporo, Japan. Environ. Sci. Technol. 41, 6920–6925. https://doi.org/10.1021/es063092m

Berrisford, P., Kållberg, P., Kobayashi, S., Dee, D., Uppala, S., Simmons, A.J., Poli, P., Sato, H. (2011). Atmospheric conservation properties in ERA-Interim. Q. J. R. Meteorolog. Soc. 137, 1381–1399. https://doi.org/10.1002/qj.864

Bock, O., Nuret, M. (2009). Verification of NWP model analyses and radiosonde humidity data with GPS precipitable water vapor estimates during AMMA.Wea. Forecasting. 24, 1085–1101. https://doi.org/10.1175/2009WAF2222239.1

Special issue in honor of Prof. David Y.H. Pui for his
"50 Years of Contribution in Aerosol Science and Technology" (VI)
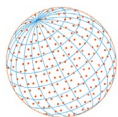
ORIGINAL RESEARCH
https://doi.org/10.4209/aaqr.220374

Boreddy, S.K.R., Kawamura, K., Jung, J. (2014). Hygroscopic properties of particles nebulized from water extracts of aerosols collected at Chichijima Island in the western North Pacific: An outflow region of Asian dust. J. Geophys. Res. 119, 167–178. https://doi.org/10.1002/2013JD020626

Buntoung, S., Janjai, S., Nunez, M., Pattarapanitchai, S., Nimnuan, P., Pariyothon, J. (2020). Spatial and temporal changes of precipitable water vapour in Thailand. Phys. Geogr. 41, 467–488. https://doi.org/10.1080/02723646.2019.1710433

Busch, B., Kandler, K., Schütz, L., Neusüß, C. (2002). Hygroscopic properties and water-soluble volume fraction of atmospheric particles in the diameter range from 50 nm to 3.8 µm during LACE 98. J. Geophys. Res. Atm. D21, 1984–2012. https://doi.org/10.1029/2000JD000228

Chakraborty, S., Guan, B., Waliser, D.E., da Silva, A.M., Uluatam, S., Hess, P. (2021). Extending the atmospheric river concept to aerosols: Climate and air quality impacts. Geophys. Res. Lett. 9, e2020GL091827. https://doi.org/10.1029/2020GL091827

Chen, L., Zhang, F., Zhang, D., Wang, X., Song, W., Liu, J., Ren, J., Jiang, S., Li, X., Li, Z. (2022). Measurement report: Hygroscopic growth of ambient fine particles measured at five sites in China. Atmos. Chem. Phys. 22, 6773–6786. https://doi.org/10.5194/acp-22-6773-2022

Chen, Y., Wild, O., Wang, Y., Ran, L., Teich, M., Größ, J., Wang, L., Spindler, G., Herrmann, H., Pinxteren, D.V., McFiggans, G., Wiedensohler, A. (2018). The influence of impactor size cut-off shift caused by hygroscopic growth on particulate matter loading and composition measurements. Atmos. Environ. 195, 141–148. https://doi.org/10.1016/j.atmosenv.2018.09.049

Choomanee, P., Bualert, S., Thongyen, T., Salao, S., Szymanski, W.W., Rungratanaubon, T. (2020). Vertical variation of carbonaceous aerosols within the $PM_{2.5}$ fraction in Bangkok, Thailand. Aerosol Air Qual. Res. 20, 43–52. https://doi.org/10.4209/aaqr.2019.04.0192

Clegg, S.L., Brimblecombe, P., Wexler, A.S. (1998). Thermodynamic model of the system $H^+–NH_4^+–Na^+–SO_4^{2-}–NO_3^-–Cl^-–H_2O$ at 298.15 K. J. Phys. Chem. 102, 2155–2171. https://doi.org/10.1021/jp973043j

Coggon, M.M., Sorooshian, A., Wang, Z., Metcalf, A.R., Frossard, A.A., Lin, J.J., Craven, J.S., Nenes, A., Jonsson, H.H., Russell, L.M., Flagan, R.C., Seinfeld, J.H. (2012). Ship impacts on the marine atmosphere: Insights into the contribution of shipping emissions to the properties of marine aerosol and clouds. Atmos. Chem. Phys. 12, 8439–8458. https://doi.org/10.5194/acp-12-8439-2012

Decesari, S., Facchini, M.C., Matta, E., Mircea, M., Fuzzi, S., Chughtai, A.R., Smith, D.M. (2002). Water soluble organic compounds formed by oxidation of soot. Atmos. Environ. 36, 1827–1832. https://doi.org/10.1016/S1352-2310(02)00141-3

Dee, D.P., Uppala, S.M., Simmons, A.J., Berrisford, P., Poli, P., Kobayashi, S., Andrae, U., Balmaseda, M.A., Balsamo, G., Bauer, P., Bechtold, P., Beljaars, A.C.M., Van De Berg, L., Bidlot, J., Bormann, N., Delsol, C., Dragani, R., Fuentes, M., Geer, A.J., Haimberger, L., et al. (2011). The ERA-Interim reanalysis: Configuration and performance of the data assimilation system. Q.J.R. Meteorol. Soc. 137, 553–597. https://doi.org/10.1002/qj.828

Fan, X., Liu, J., Zhang, F., Chen, L., Collins, D., Xu, W., Jin, X., Ren, J., Wang, Y., Wu, H., Li, S., Sun, Y., Li, Z. (2020). Contrasting size-resolved hygroscopicity of fine particles derived by HTDMA and HR-ToF-AMS measurements between summer and winter in Beijing: The impacts of aerosol aging and local emissions. Atmos. Chem. Phys. 20, 915–929. https://doi.org/10.5194/acp-20-915-2020

Gu, J., Bai, Z., Liu, A., Wu, L., Xie, Y., Li, W., Dong, H., Zhang, X. (2010). Characterization of atmospheric organic carbon and element carbon of $PM_{2.5}$ and PM_{10} at Tianjin, China. Aerosol Air Qual. Res. 10, 167–176. https://doi.org/10.4209/aaqr.2009.12.0080

Hansson, H.C., Bhend, J. (2015). Causes of Regional Change—Aerosols, in: The BACC II Author Team (Ed.), Second Assessment of Climate Change for the Baltic Sea Basin, Springer International Publishing, Cham, pp. 441–452. https://doi.org/10.1007/978-3-319-16006-1_24

Heintzenberg, J., Covert, D.C., Dingenen, R.V. (2000). Size distribution and chemical composition of marine aerosols: A compilation and review. Tellus Ser. B 52, 1104–1122. https://doi.org/10.3402/tellusb.v52i4.17090

Hsiao, T.C., Ye, W. C., Wang, S.H., Tsay, S.C., Chen, W. N., Lin, N.H., Lee, C.T., Hung, H.M., Chuang, M.T., Chantara, S. (2016). Investigation of the CCN activity, BC and UVBC mass concentrations of biomass burning aerosols during the 2013 BASELInE campaign. Aerosol Air Qual. Res. 16, 2742–2756. https://doi.org/10.4209/aaqr.2015.07.0447

Special issue in honor of Prof. David Y.H. Pui for his
"50 Years of Contribution in Aerosol Science and Technology" (VI)

ORIGINAL RESEARCH
https://doi.org/10.4209/aaqr.220374

Intergovernmental Panel on Climate Change (IPCC) (2013). The physical science basis. in: Stocker, T.F., Qin, D., Plattner, G.K., Tignor, M., Allen, S.K., Boschung, J., Nauels, A., Xia, Y., Bex, V., Midgley, P.M. (Eds.), Contribution of Working Group I to the Fifth Assessment Report of the Intergovernmental Panel on Climate Change, Climate change. Cambridge University Press, Cambridge and New York, NY. 1535.

Jiang, R., Tan, H., Tang, L., Cai, M., Yin, Y., Li, F., Liu, L., Xu, H., Chan, P. W., Deng, X., Wu, D. (2016). Comparison of aerosol hygroscopicity and mixing state between winter and summer seasons in Pearl River Delta region, China. Atmos. Res. 169, 160–170. https://doi.org/10.1016/j.atmosres.2015.09.031

Jing, B., Wang, Z., Tan, F., Guo, Y., Tong, S., Wang, W., Zhang, Y., Ge, M. (2018). Hygroscopic behavior of atmospheric aerosols containing nitrate salts and water-soluble organic acids. Atmos. Chem. Phys. 1, 5115–5127. https://doi.org/10.5194/acp-18-5115-2018

Karagulian, F., Belis, C.A., Dora, C.F.C., Prüss-Ustün, A.M., Bonjour, S., Adair-Rohani, H., Amann, M. (2015). Contributions to cities' ambient particulate matter (PM): A systematic review of local source contributions at global level. Atmos. Environ. 120, 475–483. https://doi.org/10.1016/j.atmosenv.2015.08.087

Keuken, M.P., Jonkers, S., Zandveld, P., Voogt, M. (2012). Elemental carbon as an indicator for evaluating the impact of traffic measures on air quality and health. Atmos. Environ. 61, 1–8. https://doi.org/10.1016/j.atmosenv.2012.07.009

Kim, N., Yum, S.S., Park, M., Park, J.S., Shin, H.J., Ahn, J.Y. (2020). Hygroscopicity of urban aerosols and its link to size-resolved chemical composition during spring and summer in Seoul, Korea. Atmos. Chem. Phys. 20, 11245–11262. https://doi.org/10.5194/acp-20-11245-2020

Laskina, O., Morris, H. S., Grandquist, J. R., Qin, Z., Stone, E. A., Tivanski, A. V., Grassian, V. H. (2015). Size matters in the water uptake and hygroscopic growth of atmospherically relevant multicomponent aerosol particles. J. Phys. Chem. 119, 4489-4497. https://doi.org/10.1021/jp510268p

Liu, P.F., Zhao, C.S., Göbel, T., Hallbauer, E., Nowak, A., Ran, L., Xu, W.Y., Deng, Z.Z., Ma, N., Mildenberger, K., Henning, S., Stratmann, F., Wiedensohler, A. (2011). Hygroscopic properties of aerosol particles at high relative humidity and their diurnal variations in the North China Plain. Atmos. Chem. Phys. 11, 3479–3494. https://doi.org/10.5194/acp-11-3479-2011

Massling, A., Wiedensohler, A., Busch, B., Neusüß, C., Quinn, P., Bates, T., Covert, D. (2003). Hygroscopic properties of different aerosol types over the Atlantic and Indian Oceans. Atmos. Chem. Phys. 3, 1377–1397. https://doi.org/10.5194/acp-3-1377-2003

Massling, A., Stock, M., Wiedensohler, A. (2005). Diurnal, weekly, and seasonal variation of hygroscopic properties of submicrometer urban aerosol particles. Atmos. Environ. 39, 3911–3922. https://doi.org/10.1016/j.atmosenv.2005.03.020

Massling, A., Stock, M., Wehner, B., Wu, Z. J., Hu, M., Brüggemann, E., Gnauk, T., Herrmann, H., Wiedensohler, A. (2009). Size segregated water uptake of the urban submicrometer aerosol in Beijing. Atmos. Environ. 43, 1578–1589. https://doi.org/10.1016/j.atmosenv.2008.06.003

McMurry, P.H., Litchy, M., Huang, P.F., Cai, X., Turpin, B.J., Dick, W.D., Hanson, A. (1996). Elemental composition and morphology of individual particles separated by size and hygroscopicity with the TDMA, Atmos. Environ. 30, 101–108. https://doi.org/10.1016/1352-2310(95)00235-Q

McMurry, P.H. (2000). A review of atmospheric aerosol measurements. Atmos. Environ. 34, 1959–1999. https://doi.org/10.1016/S1352-2310(99)00455-0

Meier, J., Wehner, B., Massling, A., Birmili, W., Nowak, A., Gnauk, T., Brüggemann, E., Herrman, H., Min, H., Wiedensohler, A. (2009). Hygroscopic growth of urban aerosol particles in Beijing (China) during wintertime: a comparison of three experimental methods. Atmos. Chem. Phys. 9, 6865–6880. https://doi.org/10.5194/acp-9-6865-2009

Mochida, M., Kuwata, M., Miyakawa, T., Takegawa, N., Kawamura, K., Kondo, Y. (2006). Relationship between hygroscopicity and cloud condensation nuclei activity for urban aerosols in Tokyo. J. Geophys. Res. 111, D23204. https://doi.org/10.1029/2005JD006980

Mochida, M., Nishita-Hara, C., Furutani, H., Miyazaki, Y., Jung, J., Kawamura, K., Uematsu, M. (2011). Hygroscopicity and cloud condensation nucleus activity of marine aerosol particles over the western North Pacific. J. Geophys. Res. 116, D6. https://doi.org/10.1029/2010JD014759

Notario, A., Bravo, I., Adame, J. A., Díaz-de-Mera, Y., Aranda, A., Rodríguez, A., Rodríguez, D. (2013). Variability of oxidants (OX= O_3+ NO_2), and preliminary study on ambient levels of

Special issue in honor of Prof. David Y.H. Pui for his
"50 Years of Contribution in Aerosol Science and Technology" (VI)

ORIGINAL RESEARCH
https://doi.org/10.4209/aaqr.220374

ultrafine particles and VOCs, in an important ecological area in Spain. Atmos. Res. 128, 35–45. https://doi.org/10.1016/j.atmosres.2013.03.008

O'Dowd, C.D., De Leeuw, G. (2007). Marine aerosol production: A review of the current knowledge. Phil. Trans. R. Soc. A 1856, 1753–1774. https://doi.org/10.1098/rsta.2007.2043

Petters, M.D., Kreidenweis, S.M. (2007). A single parameter representation of hygroscopic growth and cloud condensation nucleus activity. Atmos. Chem. Phys. 7, 1961-1971. https://doi.org/10.5194/acp-7-1961-2007

Raes, F., Van Dingenen, R., Vignati, E., Wilson, J., Putaud, J.P., Seinfeld, J.H., Adams, P. (2000). Formation and cycling of aerosols in the global troposphere. Atmos. Environ. 34, 4215–4240. https://doi.org/10.1016/S1474-8177(02)80021-3

Riemer, N., Ault, A.P., West, M., Craig, R.L., Curtis, J.H. (2019). Aerosol mixing state: Measurements, modeling, and impacts. Rev. Geophys. 57, 187–249. https://doi.org/10.1029/2018RG000615

Rienecker, M.M., Suarez, M.J., Todling, R., Bacmeister, J., Takacs, L., Liu, H.C., Gu, W., Sienkiewicz, M., Koster, R.D., Gelaro, R., Stajner, I., Nielsen, J.E. (2008). The GEOS-5 data assimilation system-documentation of versions 5.0.1, 5.1.0, and 5.2.0. Technical Report Series on Global Modeling and Data Assimilation, Volume 27. NASA/TM-2008-104606. https://ntrs.nasa.gov/api/citations/20120011955/downloads/20120011955.pdf

Rungratanaubon, T., Sutum, V., Bualert, S. (2017). Hygroscopic properties of fine particulate matter on sub-urban upper northern Thailand. J. Assoc. Res. 22, 143–153. https://so04.tci-thaijo.org/index.php/jar/article/view/242923

Sakamoto, K.M., Allan, J.D., Coe, H., Taylor, J.W., Duck, T.J., Pierce, J.R. (2015). Aged boreal biomass-burning aerosol size distributions from BORTAS 2011. Atmos. Chem. Phys. 15, 1633–1646. https://doi.org/10.5194/acp-15-1633-2015

Salma, I., Borsós, T., Weidinger, T., Aalto, P., Hussein, T., Dal Maso, M., Kulmala, M. (2011). Production, growth and properties of ultrafine atmospheric aerosol particles in an urban environment. Atmos. Chem. Phys. 11, 1339–1353. https://doi.org/10.5194/acp-11-1339-2011

Sumner, G.N. (1988). Precipitation Process and Analysis. John. Wiley. 455, New York.

Svenningsson, B., Hansson, H. C., Wiedensohler, A., Noone, K., Ogren, J., Hallberg, A., Colvile, R. (1994). Hygroscopic growth of aerosol particles and its influence on nucleation scavenging in cloud: Experimental results from Kleiner Feldberg. J. Atmos. Chem. 19, 129–152. https://doi.org/10.1007/978-94-011-0313-8_7

Svenningsson, B., Hansson, H.C., Martinsson, B., Wiedensohler, A., Swietlicki, E., Cederfelt, S.I., Wendisch, M., Bower, K.N., Choularton, T.W., Colvile, R.N. (1997). Cloud droplet nucleation scavenging in relation to the size and hygroscopic behaviour of aerosol particles. Atmos. Environ. 31, 2463–2475. https://doi.org/10.1016/S1352-2310(96)00179-3

Swietlicki, E., Zhou, J., Berg, O.H., Martinsson, B.G., Frank, G., Cederfelt, S.I., Dusek, U., Berner, A., Birmili, W., Wiedensohler, A., Yuskiewicz, B., Bower, K.N. (1999). A closure study of sub-micrometer aerosol particle hygroscopic behaviour. Atmos. Res. 50, 205–240. https://doi.org/10.1016/S0169-8095(98)00105-7

Swietlicki, E., Hansson, H. C., Hämeri, K., Svenningsson, B., Massling, A., McFiggans, G., Mcmurry, P.H., Petäjä, T., Tunved, P., Gysel, M., Topping, D., Weingartner, E., Baltensperger, U., Rissler, J., Wiedensohler, A., Kulmala, M. (2008). Hygroscopic properties of sub-micrometer atmospheric aerosol particles measured with H-TDMA instruments in various environments a review. Tellus B 60, 432–469. https://doi.org/10.1111/j.1600-0889.2008.00350.x

Tan, H., Yin, Y., Gu, X., Li, F., Chan, P.W., Xu, H., Deng, X., Wan, Q. (2013). An observational study of the hygroscopic properties of aerosols over the Pearl River Delta region. Atmos. Environ. 77, 817–826. https://doi.org/10.1016/j.atmosenv.2013.05.049

Tschiersch, J., Busch, B., Fogh, C.L. (1997). Measurements of concentration, size distribution and hygroscopicity of Munich winter aerosol. J. Aerosol. Sci. 28, S209–S210. https://doi.org/10.1016/s0021-8502(97)85105-1

Tunguraiwan, K. (2009). Variation of concentrations and chemical compositions of PM_{10} in Samutprakarn province. MSc thesis. Chulalongkorn University, Thailand.

Vu, T.V., Delgado-Saborit, J.M., Harrison, R.M. (2015). A review of hygroscopic growth factors of submicron aerosols from different sources and its implication for calculation of lung deposition efficiency of ambient aerosols. Air Qual. Atmos. Health. 8, 429–440. https://doi.org/10.1007/s11869-015-0365-0

Special issue in honor of Prof. David Y.H. Pui for his
"50 Years of Contribution in Aerosol Science and Technology" (VI)

ORIGINAL RESEARCH
https://doi.org/10.4209/aaqr.220374

Vu, T.V., Shi, Z., Harrison, R.M. (2021). Estimation of hygroscopic growth properties of source-related sub-micrometre particle types in a mixed urban aerosol. NPJ Clim. Atmos. Sci. 1, 1–8. https://doi.org/10.1038/s41612-021-00175-w

Wang, H., Zhu, B., Shen, L., An, J., Yin, Y., Kang, H. (2014). Number size distribution of aerosols at Mt. Huang and Nanjing in the Yangtze River Delta, China: Effects of air masses and characteristics of new particle formation. Atmos. Res. 150, 42–56. https://doi.org/10.1016/j.atmosres.2014.07.020

Wang, X., Shen, X.J., Sun, J.Y., Zhang, X.Y., Wang, Y.Q., Zhang, Y.M., Wang, P., Xia, C., Qi, X.F., Zhong, J.T. (2018). Size-resolved hygroscopic behavior of atmospheric aerosols during heavy aerosol pollution episodes in Beijing in December 2016. Atmos. Environ. 194, 188–197. https://doi.org/10.1016/j.atmosenv.2018.09.041

Wang, X., Lei, H., Berger, R., Zhang, Y., Su, H., Cheng, Y. (2020). Hygroscopic properties of NaCl nanoparticles on the surface: A scanning force microscopy study. Phys. Chem. Chem. Phys. 22, 9967–9973. https://doi.org/10.1039/D0CP00155D

Watson, J.G., Chow, J.C., Chen, L.W.A. (2005). Summary of organic and elemental carbon/black carbon analysis, methods and interpretations. Aerosol Air Qual. Res. 5, 65–102. https://doi.org/10.4209/aaqr.2005.06.0006

Wexler, A.S., Clegg, S.L. (2002). Atmospheric aerosol models for systems including the ions H$^+$, NH$_4^+$, Na$^+$, SO$_4^{2-}$, NO$_3^-$, Cl$^-$, Br$^-$, and H$_2$O. J. Geophys. Res. 107, ACH 14-1–ACH 14-14. https://doi.org/10.1029/2001JD000451

Willeke, K., Whitby, K.T. (1975). Atmospheric aerosols: Size distribution interpretation. J. Air Pollut. Control Assoc. 25, 529–534. https://doi.org/10.1080/00022470.1975.10470110

Won, W.S., Oh, R., Lee, W., Ku, S., Su, P.C., Yoon, Y.J. (2021). Hygroscopic properties of particulate matter and effects of their interactions with weather on visibility. Sci. Rep. 11, 1–12. https://doi.org/10.1038/s41598-021-95834-6

Wu, Z.J., Poulain, L., Henning, S., Dieckmann, K., Birmili, W., Merkel, M., van Pinxteren, D., Spindler, G., Müller, K., Stratmann, F., Herrmann, H., Wiedensohler, A. (2013). Relating particle hygroscopicity and CCN activity to chemical composition during the HCCT-2010 field campaign. Atmos. Chem. Phys. 13, 7983–7996. https://doi.org/10.5194/acp-13-7983-2013

Wu, Z.J., Zheng, J., Shang, D.J., Du, Z.F., Wu, Y.S., Zeng, L.M., Wiedensohler, A., Hu, M. (2016). Particle hygroscopicity and its link to chemical composition in the urban atmosphere of Beijing, China, during summertime, Atmos. Chem. Phys. 16, 1123–1138. https://doi.org/10.5194/acp-16-1123-2016

Xu, W., Ovadnevaite, J., Fossum, K. N., Lin, C., Huang, R.J., O'Dowd, C., Ceburnis, D. (2020). Aerosol hygroscopicity and its link to chemical composition in the coastal atmosphere of Mace Head: Marine and continental air masses. Atmos. Chem. Phys. 20, 3777–3791. https://doi.org/10.5194/acp-20-3777-2020

Ye, X., Stock, M., Wehner, B., Wu, Z.J., Hu, M., Bruggemann, E., Gnauk, T., Herrmann, H., Wiedensohler, A. (2009). Size segregated water uptake of the urban submicrometer aerosol in Beijing. Atmos. Environ. 43, 1578–1589. https://doi.org/10.1016/j.atmosenv.2008.06.003

Ye, X., Ma, Z., Hu, D., Yang, X., Chen, J. (2011). Size-resolved hygroscopicity of submicrometer urban aerosols in Shanghai during wintertime. Atmos. Res. 99, 353–364. https://doi.org/10.1016/j.atmosres.2010.11.008

Ye, X., Tang, C., Yin, Z., Chen, J., Ma, Z., Kong, L., Yang, X., Gao, W., Geng, F. (2013). Hygroscopic growth of urban aerosol particles during the 2009 Mirage-Shanghai Campaign. Atmos. Environ. 64, 263–269. https://doi.org/10.1016/j.atmosenv.2012.09.064

Zappoli, S., Andracchio, A., Fuzzi, S., Facchini, M. C., Gelencser, A., Kiss, G., Krivácsy, Z., Molnár, Á., Mészáros, E., Hansson, H.C., Rosman, K., Zebühr, Y. (1999). Inorganic, organic and macromolecular components of fine aerosol in different areas of Europe in relation to their water solubility. Atmos. Environ. 33, 2733–2743. https://doi.org/10.1016/S1352-2310(98)00362-8

Zhang, F., Bei, N., Nielsen-Gammon, J.W., Li, G., Zhang, R., Stuart, A., Aksoy, A. (2007). Impacts of meteorological uncertainties on ozone pollution predictability estimated through meteorological and photochemical ensemble forecasts. J. Geophys. Res. 112, D04304. https://doi.org/10.1029/2006JD007429

Zhang, F., Wang, Y., Peng, J., Ren, J., Collins, D., Zhang, R., Sun, Y., Yang, X., Li, Z. (2017). Uncertainty in predicting CCN activity of aged and primary aerosols. J. Geophys. Res. 122,

11723–11736. https://doi.org/10.1002/2017JD027058
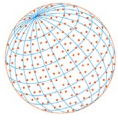
Zhang, Q., Ye, J., Zhang, S., Han, F. (2018). Precipitable water vapor retrieval and analysis by multiple data sources: Ground-based GNSS, radio occultation, radiosonde, microwave satellite, and NWP reanalysis data. J. Sens. 2018, e3428303. https://doi.org/10.1155/2018/3428303

Zieger, P., Fierz-Schmidhauser, R., Weingartner, E., Baltensperger, U. (2013). Effects of relative humidity on aerosol light scattering: results from different European sites. Atmos. Chem. Phys. 13, 10609–10631. https://doi.org/10.5194/acp-13-10609-2013